Noname manuscript No.
(will be inserted by the editor)

Shape Optimization of an Electrostatic Capacitive Sensor

Masayoshi Satake · Noboru Maeda · Shinji Fukui · Hideyuki Azegami

Received: date / Accepted: date

Abstract This paper describes the shape optimization of an electrostatic capacitive sensor used to detect fingers. We consider two state determination problems. The first is a basic electrostatic field problem consisting of sensing electrodes, an earth electrode, and air. The second is an electrostatic field problem in which fingers are added to the basic electrostatic field problem. An objective cost function is defined using the negative-signed squared H^1-norm of the difference between the solutions of the two state determination problems. The volume of the sensing electrode is used as the cost function. Using the solutions of the two state determination problems and the two adjoint problems, we present a method for evaluating the shape derivative of the objective cost function. To solve the shape optimization problem and minimize the negative-signed difference norm under the volume constraint, we use an iterative algorithm based on the H^1 gradient method. An algorithm for the shape optimization problem is developed to solve the boundary value prob-

M. Satake · H. Azegami
Graduate School of Information Science, Nagoya University, A4-2 (780) Furo-cho, Chikusa-ku, Nagoya 464-8601, Japan
E-mail: satake@az.cs.is.nagoya-u.ac.jp

H. Azegami
E-mail: azegami@is.nagoya-u.ac.jp

M. Satake · N. Maeda · S. Fukui
Nippon Soken, Inc., 14, Iwaya, Shimohasumi-cho, Nishio 445-0012, Japan
E-mail: masayoshi_satake@soken1.denso.co.jp

N. Maeda
E-mail: noboru_maeda@soken1.denso.co.jp

S. Fukui
E-mail: shinji_fuki@soken1.denso.co.jp

lems. Numerical examples show that reasonable shapes are obtained using the present approach.

Keywords Shape optimization · Electromagnetics · Electrostatic capacitive sensor · Shape derivative · H^1 gradient method

1 Introduction

In the development of automobiles, the design of electronic devices is becoming increasingly important. In the 1960s, the only electronic devices incorporated in automobiles were alternators, but in recent years, the range of devices has expanded to include navigation systems, hybrid systems, various intelligent transport systems (ITS), and sensor devices.

To satisfy the changing needs of customers, it has become important to shorten the development period. To achieve this, computer-aided engineering (CAE) systems have been employed not only in the design of mechanical parts, but also in the design of electronic devices. In recent years, there have also been attempts to optimize these designs using CAE systems. Among the electronic devices selected for optimization, capacitive sensors have been chosen because their shape affects performance factors such as their sensitivity and signal-to-noise ratio.

Research on the optimum design of capacitive sensors began in the 1990s. The size of a capacitive sensor was optimized analytically [13]. In that study, the ratio of the size of the movable electrode to that of the fixed electrode was selected as a design variable. The sensitivity of the sensor and the signal-to-noise ratio were chosen as the cost functions. The optimum ratio of the size of the electrode to the size of the diaphragm was obtained as a function of the input capacitance of the amplifier.

In another study that attempted to optimize the capacitive pressure sensor, the linearity of capacitance with respect to pressure was chosen as the cost function, and the radius of the electrode was used as the design variable [8]. A touch sensor was optimized by choosing the offset position of the electrode as the design variable and the sensitivity of the touch sensor as the objective cost function [10]. The nonparametric optimization of electronic capacitors was achieved by defining the shape of the dielectric using a level set method [11]. Here, the term of "nonparametric" is used as the meaning of "of distributed parameter" or "functional'. In the level set method, a level set function is used as a design variable to determine the boundary in the Euler description. The capacitance energy of the electric capacitor was chosen as the cost function, and the optimum shape of the capacitor was obtained using two-dimensional finite-element analysis.

A nonparametric method to optimize the shape of the domain in boundary value problems was presented by the authors. This solution was originally known as the traction method [1,6], but we have recently referred to it as the H^1 gradient method of domain variation type, because a density-variation-type H^1 gradient method has been developed for a topology optimization

Table 1 Rules and definitions for notation

Symbol	Meaning / definition
a, α, $\cdots$	Small letters mean $\mathbb{R}$ values or $\mathbb{R}$ valued functions.
$\boldsymbol{a}$, $\boldsymbol{\alpha}$, $\cdots$	Bold letters mean $\mathbb{R}^d$ values or $\mathbb{R}^d$ valued functions.
$\boldsymbol{A}$, $\boldsymbol{\Gamma}$, $\cdots$	Bold capital letters mean $\mathbb{R}^{d\times d}$ values or $\mathbb{R}^{d\times d}$ valued functions.
A, Γ, $\cdots$	Capital letters mean sets.
a_{finger}, X_{F}, $\cdots$	Subscripts of roman type mean informative labels.
$L^p\left(\Omega;\mathbb{R}^d\right)$	denotes the set of functions defined in Ω and having values in $\mathbb{R}^d$ that are $p\in[1,\infty]$-th order Lebesgue integrable.
$W^{k,p}\left(\Omega;\mathbb{R}^d\right)$	denotes the set of functions that are $k\in[0,\infty]$ times differentiable and $p\in[1,\infty]$-th order Lebesgue integrable.
$H^p\left(\Omega;\mathbb{R}^d\right)$	means $W^{2,p}\left(\Omega;\mathbb{R}^d\right)$
$\|\boldsymbol{x}\|_{H^p\left(\Omega;\mathbb{R}^d\right)}$	denotes the norm of $\boldsymbol{x}$ in $H^p\left(\Omega;\mathbb{R}^d\right)$.
$\mathscr{L}$	denotes the Lagrange function.
c , c_{finger}, $\cdots$	denote electrostatic capacitances.
u , u_{F}	denote electric potentials.
$\boldsymbol{e}$, $\boldsymbol{e}_{\mathrm{F}}$	denote electric fields.
v_0 , $v_{\mathrm{F}0}$	denote the adjoint electric potentials.
$\boldsymbol{\phi}$	denotes a domain variation (displacement) from an initial domain.
$\boldsymbol{\varphi}$	denotes a variation of $\boldsymbol{\phi}$.

problem [4]. The primary advantages of this method and a comparison with other techniques were presented in a different paper [7]. Although this approach is applicable to the design of electromagnetic devices, no such study has been published.

In the present paper, we propose a cost function that represents the performance of an electrostatic capacitive sensor, and we demonstrate the applicability of the H^1 gradient method to the nonparametric optimization of the shape of an electrostatic capacitive sensor. To define the cost function, we set two state determination problems. The first is an electrostatic field problem that consists of a sensing electrode with a certain electric potential, an earth electrode, and air. The second is similar, but has the additional consideration of fingers. As an objective cost function, we use the negative-signed squared H^1-norm of the difference between the solutions of these two state determination problems. The volume of the sensing electrode is used as the cost function.

To explain our approach to optimizing the shape of electrostatic capacitive sensors, we present our research in the following order. In Section 2, we observe the operating principle of electrostatic capacitive sensors, and construct a mathematical model of the sensor. Based on this model, we define the initial domain of an electrostatic field and the domain variation in Section 3. In Section 4, we use Maxwell's equations to formulate the two state determination problems in the varying domain. In Section 5, using the solutions to the two state determination problems, we formulate a shape optimization problem using the negative-signed squared H^1 norm of the difference between the two solutions to the state determination problems as an objective cost function, and the volume of the sensing electrode as another cost function. Methods for evaluating the Fréchet derivatives of the cost functions with respect to

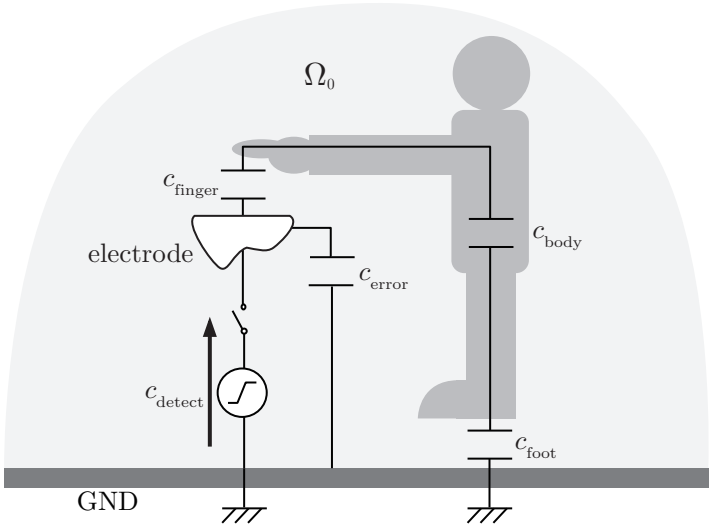

Fig. 1 Equivalent circuit of the capacitive touch sensor based on GND potential

the variation of the domain (the shape derivatives of the cost functions) are presented in Section 6. Using these shape derivatives, Section 7 describes a method to obtain the domain variations that decrease the cost functions. A scheme to solve the shape optimization problem with constraints is presented in Section 8. Finally, in Section 9, we show the numerical results of optimizing the shapes of electrostatic capacitive sensors.

In the present paper, many symbols are used to describe the electrostatic field and the domain variation. The notation is presented in Table 1. We use $\mathbb{R}$ to denote the set of real numbers and $d \in \{2, 3\}$ for the dimension number of the domains.

2 Operating principle of electrostatic capacitive sensors

First, we clarify the operating principle of an electrostatic capacitive touch sensor for detecting a human finger [9]. Figure 1 shows an equivalent circuit considered in this paper to the sensor based on GND potential. The touch sensor measures the capacitance c_{detect} (see Fig. 1), and discriminates between the touched and untouched states by detecting a change in capacitance. In this

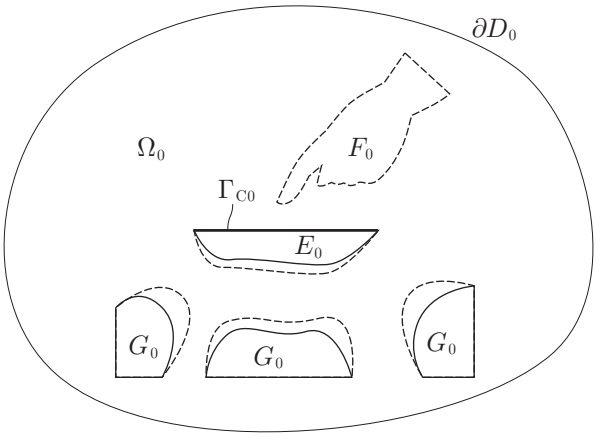

Fig. 2 Initial domain $\Omega_0 = D_0 \setminus \left(\bar{E}_0 \cup \bar{G}_0\right)$ for the electrostatic field problem

circuit, the detecting capacitance c_{detect} is given by

$$\begin{aligned} c_{\text{detect}} &= \frac{1}{\dfrac{1}{c_{\text{finger}}} + \dfrac{1}{c_{\text{body}}} + \dfrac{1}{c_{\text{foot}}}} + c_{\text{error}} \\ &= c_{\text{finger}} \frac{1}{1 + \dfrac{c_{\text{finger}}}{c_{\text{body}}} + \dfrac{c_{\text{finger}}}{c_{\text{foot}}}} + c_{\text{error}}, \end{aligned} \tag{2.1}$$

where c_{finger}, c_{body}, c_{foot}, and c_{error} are the capacitance between the electrode and finger, the capacitance of the human body, the capacitance between the human body and GND, and the error capacitance that is based on the electrostatic coupling between surrounding conductors, respectively. From measurements in a real environment, we estimated that $c_{\text{finger}} < 1$ [pF], $c_{\text{body}} > 100 \sim 1000$ [pF], and $c_{\text{foot}} > 200$ [pF] when wearing shoes. Therefore, substituting $c_{\text{finger}} \ll c_{\text{body}}$ and $c_{\text{finger}} \ll c_{\text{foot}}$ into (2.1), we can assume

$$c_{\text{detect}} \approx c_{\text{finger}} + c_{\text{error}}. \tag{2.2}$$

This approximation means that the finger has the GND potential. Moreover, as c_{error} is difficult to evaluate through simulations, c_{finger} is chosen as the first maximization target to increase the performance of the electrostatic capacitive touch sensor. To maximize c_{finger}, we develop a mathematical model of an electrostatic capacitive sensor and define a shape optimization problem using appropriate cost functions in Section 5.

3 Mathematical modeling

Based on the operating principle of an electrostatic capacitive sensor, we formulate a mathematical model of the sensor in the following way.

Figure 2 shows the initial domains for the electrostatic field. Let D_0 be a $d\,(\in\{2,3\})$-dimensional bounded domain (open set) in which electrostatic fields are permitted. In the present paper, we use the notation that ∂D_0 is the boundary of D_0 and $\bar{D}_0$ is $D_0 \cup \partial D_0$. Moreover, let $\bar{E}_0$, $\bar{G}_0$, and $\bar{F}_0$ be non-overlapping subsets of D_0 for the initial domains of a sensing electrode with a given positive electric potential, an earth electrode with zero electric potential, and a detection object with zero electric potential, respectively. Based on these definitions, we assume $\Omega_0 = D_0 \setminus \left(\bar{E}_0 \cup \bar{G}_0\right)$ is the initial domain of the electrostatic field. To define a shape optimization problem for Ω_0, its boundary $\partial\Omega_0$ must be at least a Lipschitz boundary.

The design variable in the shape optimization of Ω_0 is defined in the following way. Let $\boldsymbol{\phi}$ be the domain variation (deformation) from the initial domain D_0. Using $\boldsymbol{\phi}$, the varied domain is created by a continuous one-to-one mapping $\boldsymbol{i}+\boldsymbol{\phi} : D_0 \to \mathbb{R}^d$ as

$$\Omega\left(\boldsymbol{\phi}\right) = \left\{ \left(\boldsymbol{i}+\boldsymbol{\phi}\right)\left(\boldsymbol{x}\right) \mid \boldsymbol{x} \in \Omega_0 \right\},$$

where $\boldsymbol{i}$ is the identity mapping. In the same manner, let $\left(\,\cdot\,\right)\left(\boldsymbol{\phi}\right)$ be defined as $\left\{ \left(\boldsymbol{i}+\boldsymbol{\phi}\right)\left(\boldsymbol{x}\right) \mid \boldsymbol{x} \in \left(\,\cdot\,\right)_0 \right\}$ for the domain variation of an initial domain $\left(\,\cdot\,\right)_0$. For a function space of the design variable $\boldsymbol{\phi}$, we set

$$X = \left\{ \boldsymbol{\phi} \in H^1\left(D_0; \mathbb{R}^d\right) \;\middle|\; \boldsymbol{\phi} = \boldsymbol{0}_{\mathbb{R}^d} \text{ on } \partial D_0 \cup \partial F_0 \cup \partial G_0 \cup \Gamma_{\mathrm{C}0} \cup \bar{\Omega}_{\mathrm{C}0} \right\} \quad (3.1)$$

in order that the Fréchet derivatives of the cost functions can be defined in the dual space of X. In (3.1), $\Gamma_{\mathrm{C}0}$ and $\bar{\Omega}_{\mathrm{C}0}$ denote a boundary and a domain, respectively, in which domain variation is fixed according to the design demands. In the case of Fig. 2, $\Gamma_{\mathrm{C}0}$ is set in order to keep a plane as a touch panel. $\bar{\Omega}_{\mathrm{C}0}$ is supposed to be used for an invariable domain. Moreover, to secure the continuous one-to-one mapping of $\boldsymbol{\phi}$, we define an admissible set of the design variable $\boldsymbol{\phi}$ as

$$\mathcal{D} = \left\{ \boldsymbol{\phi} \in X \cap W^{1,\infty}\left(\mathbb{R}^d; \mathbb{R}^d\right) \;\middle|\; \|\boldsymbol{\phi}\|_{W^{1,\infty}\left(\mathbb{R}^d;\mathbb{R}^d\right)} < \sigma \right\}, \quad (3.2)$$

where σ is a positive constant such that the inverse mapping of $\boldsymbol{i}+\boldsymbol{\phi}$ becomes a continuous one-to-one mapping ([12] p. 23 Proposition 1.41).

4 State determination problems

Using the above definitions, let us define the state determination problems for an electrostatic capacitive sensor.

In an electrostatic or magnetostatic field, Maxwell's equations result in the independent Poisson equations of the electric or magnetic fields, respectively. Here, we introduce the electric potential $u : \Omega\left(\boldsymbol{\phi}\right) \to \mathbb{R}$. Then, using the constitutive equation of the electric field, we have

$$-\Delta u = \boldsymbol{\nabla} \cdot \boldsymbol{e}\left(u\right) = \frac{\rho}{\varepsilon} \quad \text{in } \Omega\left(\boldsymbol{\phi}\right), \quad (4.1)$$

where $\boldsymbol{e}(u) = -\boldsymbol{\nabla} u$ is the electric field, and ρ and ε denote the space charge density and the electric permittivity, respectively.

In the design process of an electrostatic capacitive sensor, the charge density of air is sufficiently small that ρ can be assumed to be 0. Then, (4.1) becomes a Laplace equation with respect to u:

$$-\Delta u = \boldsymbol{\nabla} \cdot \boldsymbol{e}(u) = 0 \quad \text{in } \Omega(\boldsymbol{\phi}). \tag{4.2}$$

Based on the definition and assumption, we define the first of the state determination problems in the following way.

Problem 1 (Basic electrostatic field) For $\boldsymbol{\phi} \in \mathcal{D}$ and a given function $u_{\mathrm{D}} : D_0 \to \mathbb{R}$, find $u : \Omega(\boldsymbol{\phi}) \to \mathbb{R}$ such that

$$\begin{aligned}
&-\boldsymbol{\nabla} \cdot \boldsymbol{e}(u) = 0 \quad \text{in } \Omega(\boldsymbol{\phi}) = D_0 \setminus \left(\bar{E}(\boldsymbol{\phi}) \cup \bar{G}(\boldsymbol{\phi})\right), \\
&\partial_\nu u = 0 \quad \text{on } \partial D_0, \\
&u = u_{\mathrm{D}} \quad \text{on } \partial E(\boldsymbol{\phi}), \\
&u = 0 \quad \text{on } \partial G(\boldsymbol{\phi}).
\end{aligned}$$

In Problem 1, we have assumed the Neumann condition on ∂D_0. The validity of this assumption was confirmed by comparing the numerical result given by a finite element method with actual measurements. We can confirm that there exists a weak solution of $\tilde{u} = u - u_{\mathrm{D}}$ in

$$U = \left\{ u \in H^1(D_0; \mathbb{R}) \;\middle|\; u = 0 \text{ on } \partial E(\boldsymbol{\phi}) \cup \partial G(\boldsymbol{\phi}) \right\}, \tag{4.3}$$

where $u_{\mathrm{D}} \in H^1\left(D_0; \mathbb{R}^d\right)$ is a function satisfying $u_{\mathrm{D}} = 0$ on $\partial G(\boldsymbol{\phi})$, by the Lax–Milgram theorem. The domain $\Omega(\boldsymbol{\phi})$ is extended to D_0 by Calderón's extension theorem. Moreover, we define the admissible set of $\tilde{u}$ by

$$\mathcal{S} = U \cap W^{1,\infty}(D_0; \mathbb{R}) \tag{4.4}$$

in order to use the H^1 gradient method to obtain the domain variation in $W^{1,\infty}\left(\mathbb{R}^d; \mathbb{R}^d\right)$ without singular points [2,5].

Problem 1 will be used as an equality constraint in the shape optimization problem derived below. We define the Lagrange function for Problem 1 as

$$\mathscr{L}_{\mathrm{N}}(\boldsymbol{\phi}, u, v) = -\int_{\Omega(\boldsymbol{\phi})} \boldsymbol{e}(u) \cdot \boldsymbol{e}(v) \, \mathrm{d}x, \tag{4.5}$$

for $\tilde{u} \in \mathcal{S}$ and $v \in U$. v was introduced as the Lagrange multiplier for Problem 1. If u is the solution of Problem 1,

$$\mathscr{L}_{\mathrm{N}}(\boldsymbol{\phi}, u, v) = 0$$

holds for all $v \in U$.

As the second state determination problem, we define the electrostatic field with the object F_0.

Problem 2 (Electrostatic field with an object) For $\boldsymbol{\phi} \in \mathcal{D}$ and the function $u_{\mathrm{D}} : D_0 \to \mathbb{R}$ used in Problem 1, find $u_{\mathrm{F}} : \Omega(\boldsymbol{\phi}) \setminus \bar{F}_0 \to \mathbb{R}$ such that

$$
\begin{aligned}
&- \boldsymbol{\nabla} \cdot \boldsymbol{e}(u_{\mathrm{F}}) = 0 \\
&\qquad \text{in } \Omega(\boldsymbol{\phi}) \setminus \bar{F}_0 = D_0 \setminus \left(\bar{E}(\boldsymbol{\phi}) \cup \bar{G}(\boldsymbol{\phi}) \cup \bar{F}_0\right), \\
&\partial_\nu u_{\mathrm{F}} = 0 \quad \text{on } \partial D_0, \\
&u_{\mathrm{F}} = u_{\mathrm{D}} \quad \text{on } \partial E(\boldsymbol{\phi}), \\
&u_{\mathrm{F}} = 0 \quad \text{on } \partial G(\boldsymbol{\phi}) \cup \partial F_0.
\end{aligned}
$$

As for Problem 1, we define

$$
U_{\mathrm{F}} = \left\{ u \in H^1(D_0; \mathbb{R}) \;\middle|\; u = 0 \text{ on } \partial E(\boldsymbol{\phi}) \cup \partial G(\boldsymbol{\phi}) \cup \partial F_0 \right\}, \tag{4.6}
$$

$$
\mathcal{S}_{\mathrm{F}} = U_{\mathrm{F}} \cap W^{1,\infty}(D_0; \mathbb{R}) \tag{4.7}
$$

as the function spaces for $\tilde{u}_{\mathrm{F}} = u_{\mathrm{F}} - u_{\mathrm{D}}$ and the Lagrange function for Problem 2 as

$$
\mathscr{L}_{\mathrm{F}}(\boldsymbol{\phi}, u_{\mathrm{F}}, v_{\mathrm{F}}) = - \int_{\Omega(\boldsymbol{\phi}) \setminus \bar{F}_0} \boldsymbol{e}(u_{\mathrm{F}}) \cdot \boldsymbol{e}(v_{\mathrm{F}}) \, \mathrm{d}x. \tag{4.8}
$$

$v_{\mathrm{F}} \in U_{\mathrm{F}}$ was introduced as the Lagrange multiplier for Problem 2. If u_{F} is the solution of Problem 2,

$$
\mathscr{L}_{\mathrm{F}}(\boldsymbol{\phi}, u_{\mathrm{F}}, v_{\mathrm{F}}) = 0
$$

holds for all $v_{\mathrm{F}} \in U_{\mathrm{F}}$.

5 Shape optimization problem

Using the solutions of the state determination problems, we now formulate the shape optimization problem for an electrostatic capacitive sensor.

As explained in Section 2, the performance of the sensor is determined by the difference in the capacitance c_{finger} between the touched and non-touched states. The difference is caused by the difference in the electric fields $\boldsymbol{e}(u)$ and $\boldsymbol{e}(u_{\mathrm{F}})$. Because the electric field is defined with the first derivative of the electric potential, the difference is evaluated using the error norm between u and u_{F} up to the first derivative. In the mathematical sense, this means the error norm in $H^1\left(\Omega(\boldsymbol{\phi}) \setminus \bar{F}_0; \mathbb{R}\right)$. Thus, we define an objective cost function as

$$
\begin{aligned}
&f_0(\boldsymbol{\phi}, u, u_{\mathrm{F}}) \\
&\quad = - \int_{\Omega(\boldsymbol{\phi}) \setminus \bar{F}_0} \left\{ c_0 (u - u_{\mathrm{F}})^2 + (\boldsymbol{e}(u) - \boldsymbol{e}(u_{\mathrm{F}})) \cdot (\boldsymbol{e}(u) - \boldsymbol{e}(u_{\mathrm{F}})) \right\} \mathrm{d}x.
\end{aligned} \tag{5.1}
$$

Here c_0 is a positive constant with the unit of $[1/\mathrm{m}^2]$ to make the unit of the first and the second terms of the integrand even. In this study, $c_0 = 1$ is assumed in order to accord with the error norm in $H^1\left(\Omega(\boldsymbol{\phi}) \setminus \bar{F}_0; \mathbb{R}\right)$.

Additionally, we confirmed that $c_0 = 0$ does not work well as an objective function.

Moreover, for the sake of reducing material costs, we define

$$f_1(\boldsymbol{\phi}) = \int_{E(\boldsymbol{\phi})} \mathrm{d}x - s_1, \tag{5.2}$$

as the cost function, where s_1 is a positive constant for which there exists some $\boldsymbol{\phi} \in \mathcal{D}$ such that $f_1(\boldsymbol{\phi}) \leq 0$. We confirmed that the electrode expands infinitely if $f_1(\boldsymbol{\phi})$ is not used as the constraint condition.

Using these cost functions, we define the shape optimization problem in the following way.

Problem 3 (Shape optimization problem) Let $\mathcal{D}$ and $\mathcal{S}$ be as defined in (3.2) and (4.7). For $\boldsymbol{\phi} \in \mathcal{D}$, let $\tilde{u} = u - u_{\mathrm{D}} \in \mathcal{S}$ and $\tilde{u}_{\mathrm{F}} = u_{\mathrm{F}} - u_{\mathrm{D}} \in \mathcal{S}$ be the solutions of Problem 1 and Problem 2. For f_0 and f_1 defined in (5.1) and (5.2), respectively, find $\Omega(\boldsymbol{\phi})$ such that

$$\min_{\boldsymbol{\phi}\in\mathcal{D}} \Big\{ f_0(\boldsymbol{\phi}, u, u_{\mathrm{F}}) \mid f_1(\boldsymbol{\phi}) \leq 0, \\ \tilde{u} \in \mathcal{S},\ \text{Problem 1},\ \tilde{u}_{\mathrm{F}} \in \mathcal{S},\ \text{Problem 2} \Big\}.$$

6 Shape derivatives of cost functions

To solve Problem 3, we will use the H^1 gradient method in the reshaping algorithm. The H^1 gradient method uses the shape derivatives of the cost functions. As the objective cost function $f_0(\boldsymbol{\phi}, u, u_{\mathrm{F}})$ contains u and u_{F}, we consider the two state determination problems as equality constraints. Hence, the Lagrange function for $f_0(\boldsymbol{\phi}, u, u_{\mathrm{F}})$ is defined as

$$\begin{aligned}
&\mathscr{L}_0(\boldsymbol{\phi}, u, v_0, u_{\mathrm{F}}, v_{\mathrm{F}0}) \\
&= f_0(\boldsymbol{\phi}, u, u_{\mathrm{F}}) + \mathscr{L}_{\mathrm{N}}(\boldsymbol{\phi}, u, v_0) - \mathscr{L}_{\mathrm{F}}(\boldsymbol{\phi}, u_{\mathrm{F}}, v_{\mathrm{F}0}) \\
&= \int_{\Omega(\boldsymbol{\phi})\setminus\bar{F}_0} \Big\{ -c_0 (u - u_{\mathrm{F}})^2 - (\boldsymbol{e}(u) - \boldsymbol{e}(u_{\mathrm{F}})) \cdot (\boldsymbol{e}(u) - \boldsymbol{e}(u_{\mathrm{F}})) \\
&\quad + \boldsymbol{e}(u_{\mathrm{F}}) \cdot \boldsymbol{e}(v_{\mathrm{F}0}) \Big\} \mathrm{d}x - \int_{\Omega(\boldsymbol{\phi})} \boldsymbol{e}(u) \cdot \boldsymbol{e}(v_0)\, \mathrm{d}x.
\end{aligned} \tag{6.1}$$

Hereafter, let $\boldsymbol{\varphi}$ denote a variation of $\boldsymbol{\phi} \in \mathcal{D}$ and be an arbitrary element in $\mathcal{D}$. Based on the definition, the shape derivative of $\mathscr{L}_0$ with respect to arbitrary variations $(\boldsymbol{\varphi}, u', v_0', u_{\mathrm{F}}', v_{\mathrm{F}0}') \in \mathcal{D} \times U^2 \times U_{\mathrm{F}}^2$ can be written as

$$\begin{aligned}
&\mathscr{L}_0'(\boldsymbol{\phi}, u, v_0, u_{\mathrm{F}}, v_{\mathrm{F}0})[\boldsymbol{\varphi}, u', v_0', u_{\mathrm{F}}', v_{\mathrm{F}0}'] \\
&\quad = \mathscr{L}_{0\boldsymbol{\phi}}(\boldsymbol{\phi}, u, v_0, u_{\mathrm{F}}, v_{\mathrm{F}0})[\boldsymbol{\varphi}] + \mathscr{L}_{0u}(\boldsymbol{\phi}, u, v_0, u_{\mathrm{F}}, v_{\mathrm{F}0})[u'] \\
&\qquad + \mathscr{L}_{0v_0}(\boldsymbol{\phi}, u, v_0, u_{\mathrm{F}}, v_{\mathrm{F}0})[v_0'] + \mathscr{L}_{0u_{\mathrm{F}}}(\boldsymbol{\phi}, u, v_0, u_{\mathrm{F}}, v_{\mathrm{F}0})[u_{\mathrm{F}}'] \\
&\qquad + \mathscr{L}_{0v_{\mathrm{F}0}}(\boldsymbol{\phi}, u, v_0, u_{\mathrm{F}}, v_{\mathrm{F}0})[v_{\mathrm{F}0}'].
\end{aligned} \tag{6.2}$$

The third and fifth terms on the right-hand side of (6.2) become 0 if u and u_{F} are solutions to Problem 1 and Problem 2, respectively. Moreover, the second term on the right-hand side of (6.2) becomes 0 if v_0 is a solution of the following problem.

Problem 4 (Adjoint problem for Problem 1) For $\boldsymbol{\phi} \in \mathcal{D}$, let u be the solution of Problem 1. Find $v_0 : \Omega(\boldsymbol{\phi}) \to \mathbb{R}$ such that

$$
\begin{aligned}
&- \boldsymbol{\nabla} \cdot \boldsymbol{e}(v_0) = 2\boldsymbol{\nabla} \cdot (\boldsymbol{e}(u) - \boldsymbol{e}(u_{\mathrm{F}})) - 2c_0 (u - u_{\mathrm{F}}) \\
&\qquad \text{in } \Omega(\boldsymbol{\phi}) \setminus \bar{F}_0 = D_0 \setminus \left(\bar{E}(\boldsymbol{\phi}) \cup \bar{G}(\boldsymbol{\phi}) \cup \bar{F}_0\right), \\
&- \boldsymbol{\nabla} \cdot \boldsymbol{e}(v_0) = 0 \quad \text{in } F_0, \\
&\partial_\nu v_0 = 0 \quad \text{on } \partial D_0, \\
&v_0 = 0 \quad \text{on } \partial E(\boldsymbol{\phi}) \cup \partial G(\boldsymbol{\phi}).
\end{aligned}
$$

The fourth term on the right-hand side of (6.2) becomes 0 if $v_{\mathrm{F}0}$ is a solution of the following problem.

Problem 5 (Adjoint problem for Problem 2) For $\boldsymbol{\phi} \in \mathcal{D}$, let u_{F} be the solution of Problem 2. Find $v_{\mathrm{F}0} : \Omega(\boldsymbol{\phi}) \setminus \bar{F}_0 \to \mathbb{R}$ such that

$$
\begin{aligned}
&- \boldsymbol{\nabla} \cdot \boldsymbol{e}(v_{\mathrm{F}0}) = 2\boldsymbol{\nabla} \cdot (\boldsymbol{e}(u) - \boldsymbol{e}(u_{\mathrm{F}})) - 2c_0 (u - u_{\mathrm{F}}) \\
&\qquad \text{in } \Omega(\boldsymbol{\phi}) \setminus \bar{F}_0 = D_0 \setminus \left(\bar{E}(\boldsymbol{\phi}) \cup \bar{G}(\boldsymbol{\phi}) \cup \bar{F}_0\right), \\
&\partial_\nu v_{\mathrm{F}0} = 0 \quad \text{on } \partial D_0, \\
&v_{\mathrm{F}0} = 0 \quad \text{on } \partial E(\boldsymbol{\phi}) \cup \partial G(\boldsymbol{\phi}) \cup \partial F_0.
\end{aligned}
$$

The first term on the right-hand side of (6.2) becomes

$$
\begin{aligned}
&\mathscr{L}_{0\boldsymbol{\phi}}(\boldsymbol{\phi}, u, v_0, u_{\mathrm{F}}, v_{\mathrm{F}0})[\boldsymbol{\varphi}] \\
&= \int_{\Omega(\boldsymbol{\phi}) \setminus \bar{F}_0} \Big[2(\boldsymbol{e}(u) - \boldsymbol{e}(u_{\mathrm{F}})) \cdot \left\{ \boldsymbol{\nabla}\boldsymbol{\varphi}^{\mathrm{T}} (\boldsymbol{e}(u) - \boldsymbol{e}(u_{\mathrm{F}})) \right\} \\
&- \boldsymbol{e}(u_{\mathrm{F}}) \cdot \left(\boldsymbol{\nabla}\boldsymbol{\varphi}^{\mathrm{T}} \boldsymbol{e}(v_{\mathrm{F}0}) \right) - \boldsymbol{e}(v_{\mathrm{F}0}) \cdot \left(\boldsymbol{\nabla}\boldsymbol{\varphi}^{\mathrm{T}} \boldsymbol{e}(u_{\mathrm{F}}) \right) \\
&+ \Big\{ -c_0 (u - u_{\mathrm{F}})^2 - (\boldsymbol{e}(u) - \boldsymbol{e}(u_{\mathrm{F}})) \cdot (\boldsymbol{e}(u) - \boldsymbol{e}(u_{\mathrm{F}})) \\
&+ \boldsymbol{e}(u_{\mathrm{F}}) \cdot \boldsymbol{e}(v_{\mathrm{F}0}) \Big\} \boldsymbol{\nabla} \cdot \boldsymbol{\varphi} \Big] \mathrm{d}x \\
&+ \int_{\Omega(\boldsymbol{\phi})} \Big\{ \boldsymbol{e}(u) \cdot \left(\boldsymbol{\nabla}\boldsymbol{\varphi}^{\mathrm{T}} \boldsymbol{e}(v_0) \right) + \boldsymbol{e}(v_0) \cdot \left(\boldsymbol{\nabla}\boldsymbol{\varphi}^{\mathrm{T}} \boldsymbol{e}(u) \right) \\
&- \boldsymbol{e}(u) \cdot \boldsymbol{e}(v_0) \boldsymbol{\nabla} \cdot \boldsymbol{\varphi} \Big\} \mathrm{d}x. \qquad (6.3)
\end{aligned}
$$

Here, we have used Proposition 1 in Appendix A and the Dirichlet conditions in Problem 1, Problem 2, Problem 4, and Problem 5.

From the results above, if u, u_{F}, v_0, and $v_{\mathrm{F}0}$ are solutions to Problem 1, Problem 2, Problem 4, and Problem 5, respectively, and if we write $f_0(\boldsymbol{\phi}, u(\boldsymbol{\phi}), u_{\mathrm{F}}(\boldsymbol{\phi}))$

as $\tilde{f}_0(\boldsymbol{\phi})$, we have

$$\begin{aligned}\tilde{f}_0'(\boldsymbol{\phi})[\boldsymbol{\varphi}] &= \mathscr{L}_{0\boldsymbol{\phi}}(\boldsymbol{\phi}, u, v_0, u_{\mathrm{F}}, v_{\mathrm{F}0})[\boldsymbol{\varphi}] = \langle \boldsymbol{g}_0, \boldsymbol{\varphi}\rangle \\ &= \int_{\Omega(\boldsymbol{\phi})\setminus\bar{F}_0} \left(\boldsymbol{G}_{0\Omega(\boldsymbol{\phi})\setminus\bar{F}_0}\cdot\boldsymbol{\nabla}\boldsymbol{\varphi}^{\mathrm{T}} + g_{0\Omega(\boldsymbol{\phi})\setminus\bar{F}_0}\boldsymbol{\nabla}\cdot\boldsymbol{\varphi}\right)\mathrm{d}x \\ &\quad + \int_{\Omega(\boldsymbol{\phi})} \left(\boldsymbol{G}_{0\Omega(\boldsymbol{\phi})}\cdot\boldsymbol{\nabla}\boldsymbol{\varphi}^{\mathrm{T}} + g_{0\Omega(\boldsymbol{\phi})}\boldsymbol{\nabla}\cdot\boldsymbol{\varphi}\right)\mathrm{d}x, \end{aligned} \tag{6.4}$$

where

$$\begin{aligned}\boldsymbol{G}_{0\Omega(\boldsymbol{\phi})\setminus\bar{F}_0} &= 2\left(\boldsymbol{e}(u)-\boldsymbol{e}(u_{\mathrm{F}})\right)\left(\boldsymbol{e}(u)-\boldsymbol{e}(u_{\mathrm{F}})\right)^{\mathrm{T}} \\ &\quad -\boldsymbol{e}(u_{\mathrm{F}})\cdot\boldsymbol{e}^{\mathrm{T}}(v_{\mathrm{F}0}) - \boldsymbol{e}(v_{\mathrm{F}0})\cdot\boldsymbol{e}^{\mathrm{T}}(u_{\mathrm{F}}), \end{aligned} \tag{6.5}$$

$$\begin{aligned}g_{0\Omega(\boldsymbol{\phi})\setminus\bar{F}_0} &= -c_0\left(u-u_{\mathrm{F}}\right)^2 - \left(\boldsymbol{e}(u)-\boldsymbol{e}(u_{\mathrm{F}})\right)\cdot\left(\boldsymbol{e}(u)-\boldsymbol{e}(u_{\mathrm{F}})\right) \\ &\quad +\boldsymbol{e}(u_{\mathrm{F}})\cdot\boldsymbol{e}(v_{\mathrm{F}0}), \end{aligned} \tag{6.6}$$

$$\boldsymbol{G}_{0\Omega(\boldsymbol{\phi})} = \boldsymbol{e}(u)\cdot\boldsymbol{e}^{\mathrm{T}}(v_0) + \boldsymbol{e}(v_0)\cdot\boldsymbol{e}^{\mathrm{T}}(u), \tag{6.7}$$

$$g_{0\Omega(\boldsymbol{\phi})} = -\boldsymbol{e}(u)\cdot\boldsymbol{e}(v_0). \tag{6.8}$$

To obtain (6.4) from (6.3), we use the identical equation $\boldsymbol{a}\cdot(\boldsymbol{B}\boldsymbol{c}) = \left(\boldsymbol{a}\boldsymbol{c}^{\mathrm{T}}\right)\cdot\boldsymbol{B}$ for $\boldsymbol{a}\in\mathbb{R}^d$, $\boldsymbol{B}\in\mathbb{R}^{d\times d}$ and $\boldsymbol{c}\in\mathbb{R}^d$, where $\boldsymbol{A}\cdot\boldsymbol{B}$ for $\boldsymbol{A}=(a_{ij})\in\mathbb{R}^{d\times d}$ and $\boldsymbol{B}=(b_{ij})\in\mathbb{R}^{d\times d}$ denotes $\sum_{(i,j)\in\{1,\cdots,d\}^2} a_{ij}b_{ij}$.

For $f_1(\boldsymbol{\phi})$, we obtain

$$f_1'(\boldsymbol{\phi})[\boldsymbol{\varphi}] = \int_{E(\boldsymbol{\phi})} \boldsymbol{\nabla}\cdot\boldsymbol{\varphi}\,\mathrm{d}x = \langle \boldsymbol{g}_1, \boldsymbol{\varphi}\rangle. \tag{6.9}$$

We call $\boldsymbol{g}_0$ and $\boldsymbol{g}_1$ the shape derivatives of f_0 and f_1, respectively.

7 The H^1 gradient method

The H^1 gradient method gives the variation in a design variable, such as the domain mapping or the density parameter that decreases the cost function, as a solution to a boundary value problem of an elliptic partial differential equation [6,4,3,2]. In the case of the shape derivative $\boldsymbol{g}_i$ of cost function $f_i(\boldsymbol{\phi})$ for $i\in\{0,1\}$, the H^1 gradient method can be described as follows.

Problem 6 (H^1 gradient method for Problem 3) Let X be a Hilbert space defined in (3.1), and let $a: X\times X\to\mathbb{R}$ be a bounded and coercive bilinear form on X such that there exist positive constants α and β that satisfy

$$a(\boldsymbol{w},\boldsymbol{z}) \le \alpha\|\boldsymbol{w}\|_X\|\boldsymbol{z}\|_X, \quad a(\boldsymbol{w},\boldsymbol{w}) \ge \beta\|\boldsymbol{w}\|_X^2$$

for all $\boldsymbol{w},\boldsymbol{z}\in X$. For $\boldsymbol{g}_i\in X'$ (dual space of X), which is a Fréchet derivative of the cost function $f(\boldsymbol{\phi})$ at $\boldsymbol{\phi}\in X$, find $\boldsymbol{\varphi}_{gi}\in X$ such that

$$a(\boldsymbol{\varphi}_{gi},\boldsymbol{w}) = -\langle \boldsymbol{g}_i, \boldsymbol{w}\rangle \tag{7.1}$$

for all $\boldsymbol{w}\in X$.

Problem 6 can be solved numerically with the standard finite-element method by considering that (7.1) is a weak form of a boundary value problem of an elliptic partial differential equation. In the present paper, we use

$$a\left(\boldsymbol{\varphi},\boldsymbol{\psi}\right)=\int_{\Omega(\boldsymbol{\phi})}\left(\boldsymbol{E}\left(\boldsymbol{\varphi}\right)\cdot\boldsymbol{E}\left(\boldsymbol{\psi}\right)+c_b\boldsymbol{\varphi}\cdot\boldsymbol{\psi}\right)\mathrm{d}x \tag{7.2}$$

for $\boldsymbol{\varphi}\in X$ and $\boldsymbol{\psi}\in X$, where

$$\boldsymbol{E}\left(\boldsymbol{\varphi}\right)=\frac{1}{2}\left(\frac{\partial\varphi_i}{\partial x_j}+\frac{\partial\varphi_j}{\partial x_i}\right)_{(i,j)\in\{1,\cdots,d\}^2},$$

and c_b is a positive constant.

If $\tilde{u}$ and $\tilde{u}_{\mathrm{F}}$ are included in $\mathcal{S}$, we can confirm that the solution $\boldsymbol{\varphi}_{g0}$ of Problem 6 belongs to $W^{1,\infty}\left(\mathbb{R}^d;\mathbb{R}^d\right)$ [2].

8 Solution to the shape optimization problem

We use an iterative method based on the H^1 gradient method to solve Problem 3. To determine the domain variation that reduces $f_0\left(\boldsymbol{\phi},u,u_{\mathrm{F}}\right)$ while satisfying $f_1\left(\boldsymbol{\phi}\right)\leq 0$, we use the solution of the following problem. In this section, we denote $f_0\left(\boldsymbol{\phi},u,u_{\mathrm{F}}\right)$ as $f_0\left(\boldsymbol{\phi}\right)$ and its shape derivative as $\boldsymbol{g}_0$.

Problem 7 (SQ approximation) For $\boldsymbol{\phi}\in\mathcal{D}$ satisfying $f_1\left(\boldsymbol{\phi}\right)\leq 0$, let $\boldsymbol{g}_0$ and $\boldsymbol{g}_1$ be given, $a\left(\cdot,\cdot\right)$ be given as in (7.2), and c_a be a positive constant to control the step size. Find $\boldsymbol{\varphi}$ such that

$$\min_{\boldsymbol{\varphi}\in X}\left\{q\left(\boldsymbol{\varphi}\right)=\frac{c_a}{2}a\left(\boldsymbol{\varphi},\boldsymbol{\varphi}\right)+\left\langle\boldsymbol{g}_0,\boldsymbol{\varphi}\right\rangle\;\middle|\;f_1\left(\boldsymbol{\phi}\right)+\left\langle\boldsymbol{g}_1,\boldsymbol{\varphi}\right\rangle\leq 0\right\}.$$

The Lagrange function of Problem 7 is defined as

$$\mathscr{L}_{\mathrm{SQ}}\left(\boldsymbol{\varphi},\lambda_1\right)=q\left(\boldsymbol{\varphi}\right)+\lambda_1\left(f_1\left(\boldsymbol{\phi}\right)+\left\langle\boldsymbol{g}_1,\boldsymbol{\varphi}\right\rangle\right),$$

where $\lambda_1\in\mathbb{R}$ is the Lagrange multiplier for the constraint $f_1\left(\boldsymbol{\varphi}\right)\leq 0$. The Karush–Kuhn–Tucker conditions for Problem 7 are given as

$$c_a a\left(\boldsymbol{\varphi},\boldsymbol{\varphi}\right)+\left\langle\boldsymbol{g}_0+\lambda_1\boldsymbol{g}_1,\boldsymbol{\varphi}\right\rangle=0, \tag{8.1}$$
$$f_1\left(\boldsymbol{\phi}\right)+\left\langle\boldsymbol{g}_1,\boldsymbol{\varphi}\right\rangle\leq 0, \tag{8.2}$$
$$\lambda_1\left(f_1\left(\boldsymbol{\phi}\right)+\left\langle\boldsymbol{g}_1,\boldsymbol{\varphi}\right\rangle\right)=0, \tag{8.3}$$
$$\lambda_1\geq 0 \tag{8.4}$$

for all $\boldsymbol{\varphi}\in X$. Here, let $\boldsymbol{\varphi}_{gi}$ for $i\in\{0,1\}$ be the solutions to Problem 6, and set

$$\boldsymbol{\varphi}_g=\boldsymbol{\varphi}_{g0}+\lambda_1\boldsymbol{\varphi}_{g1}. \tag{8.5}$$

Then, by substituting $\boldsymbol{\varphi}_g$ of (8.5) for $\boldsymbol{\varphi}$ in (8.1), we can see that (8.1) holds. If the constraint in (8.2) is active, i.e., (8.2) holds with the equality, we have

$$\langle \boldsymbol{g}_1, \boldsymbol{\varphi}_{g1} \rangle \lambda_1 = -f_1(\boldsymbol{\phi}) + \langle \boldsymbol{g}_1, \boldsymbol{\varphi}_{g0} \rangle . \tag{8.6}$$

Equation (8.6) has a unique solution for λ_1. Moreover, if $f_1(\boldsymbol{\phi}) = 0$, we have

$$\langle \boldsymbol{g}_1, \boldsymbol{\varphi}_{g1} \rangle \lambda_1 = -\langle \boldsymbol{g}_1, \boldsymbol{\varphi}_{g0} \rangle . \tag{8.7}$$

Because (8.7) is independent of the magnitude of $\boldsymbol{\varphi}_{g0}$ and $\boldsymbol{\varphi}_{g1}$, we determine λ_1 using (8.7) in the numerical scheme for the initial domain Ω_0, where we assume $f_1(\boldsymbol{\phi}) = 0$ is satisfied. If $\lambda_1 < 0$ in the solution to (8.6) or (8.7), we can set $\lambda_1 = 0$ to satisfy (8.1)–(8.4).

The numerical scheme is described below.

1. Set Ω_0 and $\boldsymbol{\phi}_0 = \boldsymbol{i}$ as $f_1(\boldsymbol{\phi}_0) \leq 0$. Set c_a, ϵ_0, and ϵ_1 appropriately. Set $k = 0$.
2. Solve Problem 1 and Problem 2 at $\boldsymbol{\phi}_k$ by a numerical method, and compute $f_0(\boldsymbol{\phi}_k)$ and $f_1(\boldsymbol{\phi}_k)$.
3. Solve Problem 4 and Problem 5 at $\boldsymbol{\phi}_k$ by a numerical method, and compute $\boldsymbol{g}_0$ and $\boldsymbol{g}_1$.
4. Solve $\boldsymbol{\varphi}_{g0}$ and $\boldsymbol{\varphi}_{gi_1}$ using

$$c_a a(\boldsymbol{\varphi}_{gi}, \boldsymbol{w}) = -\langle \boldsymbol{g}_i, \boldsymbol{w} \rangle$$

   for all $\boldsymbol{w} \in X$ by a numerical method.
5. Solve λ_{1k+1} using (8.7) when $k = 0$ and (8.6) when $k > 0$.
6. Compute $\boldsymbol{\varphi}_g$ using (8.5), set $\boldsymbol{\phi}_{k+1} = \boldsymbol{\phi}_k + \boldsymbol{\varphi}_g$, and compute $f_0(\boldsymbol{\phi}_{k+1})$ and $f_1(\boldsymbol{\phi}_{k+1})$.
7. Assess $|f_0(\boldsymbol{\phi}_{k+1}) - f_0(\boldsymbol{\phi}_k)| \leq \epsilon_0$.
   - If the condition in step 6 holds, proceed to step 8.
   - If not, replace $k+1$ with k and return to step 3.
8. Stop the algorithm.

9 Numerical examples

In the present study, we developed a computer program in JAVA API using the commercial software package COMSOL Multiphysics to solve the boundary value problems. With this program, we solved two types of problems. The first type consisted of plain plates for the earth electrode G_0 and the detection object F_0 located in parallel. The second type consisted of a protruding shaped G_0 and a stick-type F_0.

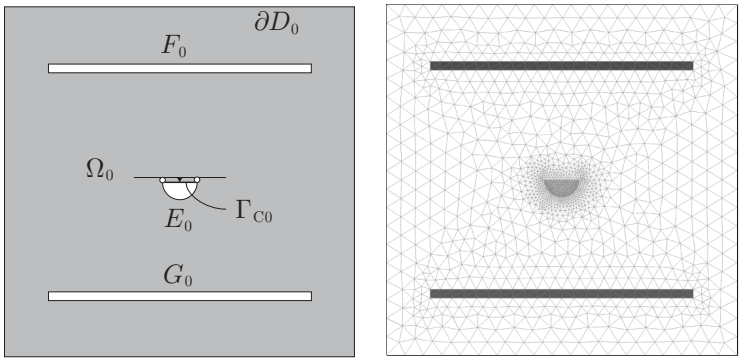

(a) Problem setting (b) Finite-element model

Fig. 3 Example 1a: Two-dimensional electrostatic field with parallel electrodes

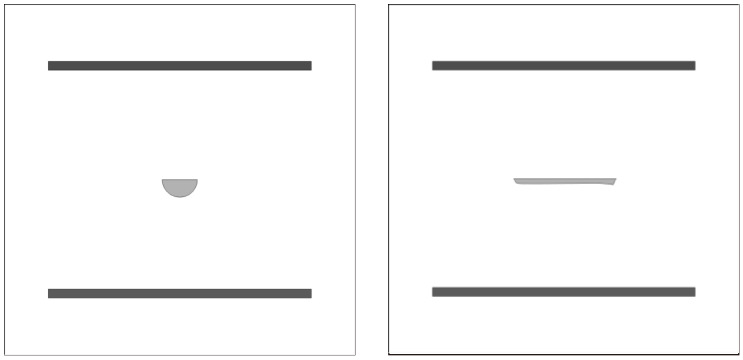

(a) Initial (b) Optimized (not converged)

Fig. 4 Example 1a: Shapes before and after domain variation

9.1 Examples of parallel electrodes

The setting and the finite-element mesh of Example 1a are shown in Fig. 3. We assumed that the domain variation was fixed in the normal direction on Γ_{C0} and fixed perfectly at the center of Γ_{C0}. Figure 4 shows the initial and optimized domains of the electrostatic field. From the problem setting, we expected that a flatter shape would result in a greater decrease in the cost function. Actually, the optimized shape shown in Fig. 4 (b) was flatter than the initial shape in Fig. 4 (a). Figures 5–6 show the iteration history of the cost functions and capacitances. From Figs. 5–6, we can confirm that f_0 decreases under constant f_1, and the difference in electrostatic capacitances with and without the finger increases. However, after the 13th iteration, we encountered some mesh distortion due to the thin shape of the electrode, and terminated the algorithm.

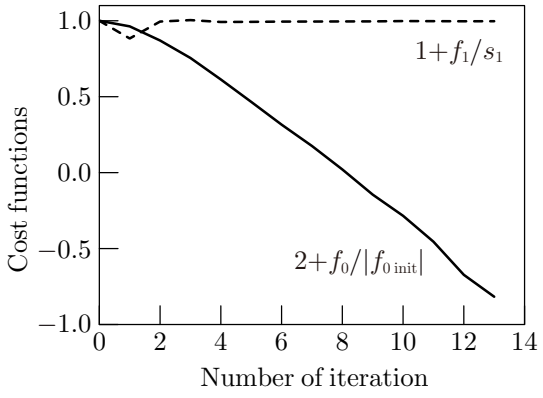

Fig. 5 Example 1a: Iteration history of cost functions

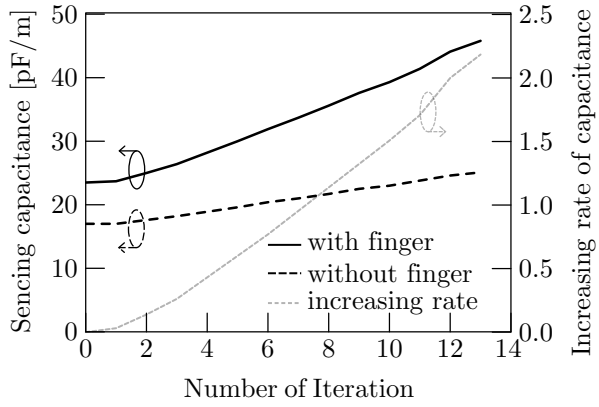

Fig. 6 Example 1a: Iteration history of sensing capacitance and rate of capacitance difference against initial shape

To obtain a converged shape, we analyzed an additional problem. Figure 7 shows the setting and the finite-element mesh of Example 1b. In this problem, the design domain of the electrode was limited to $D_0 \setminus \bar{\Omega}_{\mathrm{C}0}$. Figure 8 shows the shapes before and after domain variation. The iteration history of the cost functions and the detected capacitance values are shown in Figs. 9–10. As expected, the cost function f_0 decreased under constant f_1, and converged after 25 iterations.

9.2 Examples of protruding electrodes

In Example 2a, we examined a more complex shape (see Fig. 11). Here, we assumed that the domain variation was fixed in the upper direction in Fig. 11 on $\Gamma_{\mathrm{C}0}$ and fixed perfectly at the center point of $\Gamma_{\mathrm{C}0}$. Figure 12 shows the shapes

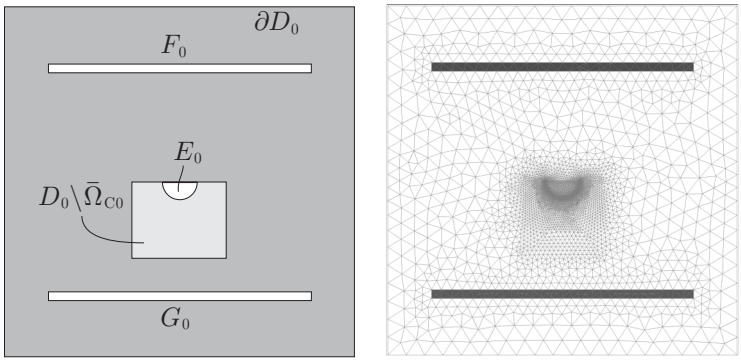

(a) Problem setting (b) Finite-element model

Fig. 7 Example 1b: Two-dimensional electrostatic field with parallel electrodes

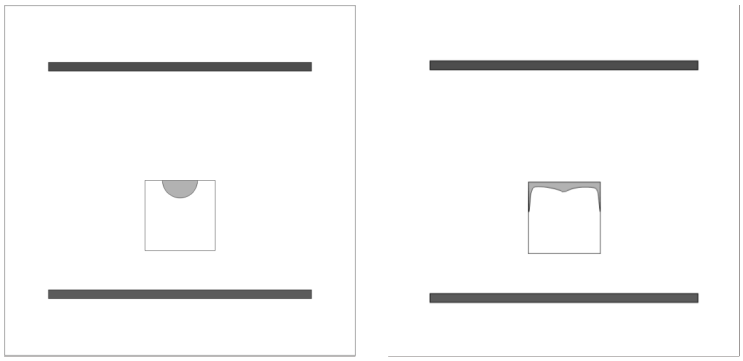

(a) Initial (b) Optimized (convergence)

Fig. 8 Example 1b: Shapes before and after domain variation

before and after domain variation. Figures 13–14 show the iteration history of the cost functions and capacitances. From Figs. 13–14, we can observe that f_0 decreased when satisfying the constraint condition $f_1 \leq 0$, and the difference in electrostatic capacitance with and without the finger increased. The optimized electrode becomes thinner, although the objective function f_0 does not converge because of the mesh distortion problem encountered in Example 1a.

Hence, we analyzed the additional example shown in Fig. 15, with the design domain of the electrode $D_0 \setminus \bar{\Omega}_{C0}$. The shape obtained by the present method is shown in Fig. 16. It is apparent that the optimized shape becomes rounded at both ends of the electrode. From the iteration history shown in Figs. 17–18, we can confirm that the cost function f_0 decreased under a constant f_1, and converged after 21 iterations. At the same time, the difference in electrostatic capacitance with and without the finger increased.

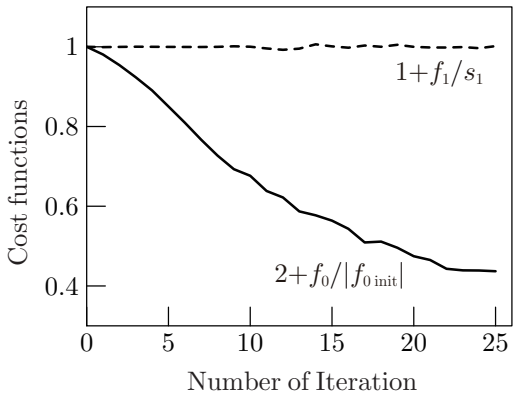

Fig. 9 Example 1b: Iteration history of cost functions

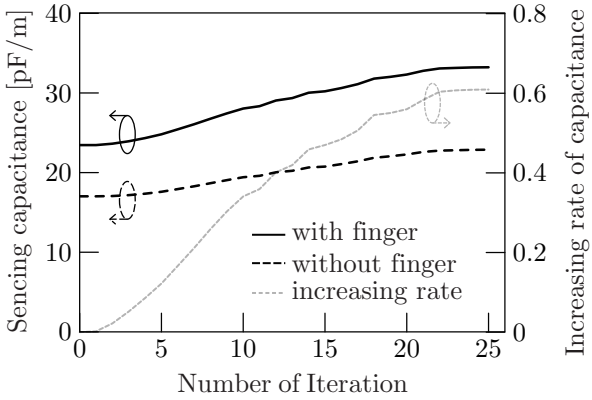

Fig. 10 Example 1b: Iteration history of sensing capacitance and rate of capacitance difference against initial shape

10 Conclusions

In this paper, we have formulated a shape optimization problem for a capacitive sensor for detecting fingers in an electrostatic field. The sensitivity of the finger detection was defined using a cost function of the negative-signed squared H^1-norm of the difference between the solutions of two state determination problems. The first problem is a basic electrostatic field problem consisting of a sensing electrode, an earth electrode, and air. The second problem considers the presence of fingers in the first problem. The volume of the sensing electrode was used as the constraint cost function. The shape derivative of the objective cost function was evaluated with the solutions of the two state determination problems and the two adjoint problems. To solve the shape optimization problem such that it minimizes the negative-signed difference norm with the volume constraint, an iterative algorithm based on the H^1

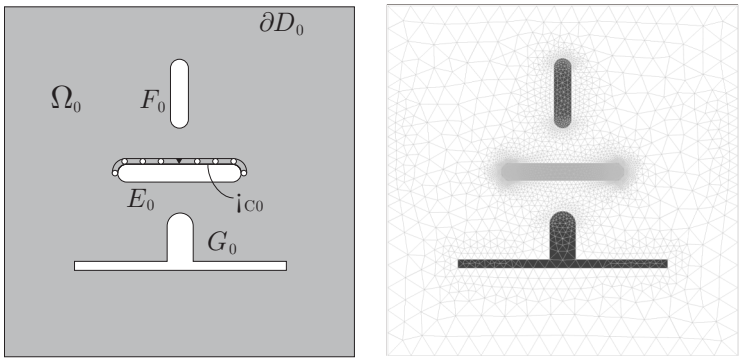

(a) Problem setting (b) Finite-element model

Fig. 11 Example 2a: Two-dimensional electrostatic field with protruding earth electrode

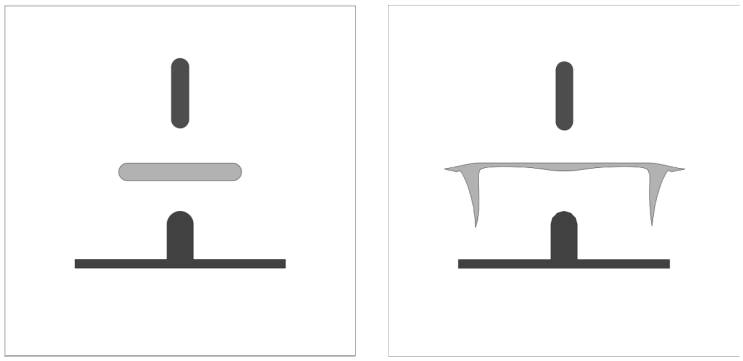

(a) Initial (b) Optimized (not converged)

Fig. 12 Example 2a: Shapes before and after domain variation

gradient method was used. A computer program was developed with JAVA API, using the commercial software package COMSOL Multiphysics to solve the boundary value problems.

In a series of numerical examples, we found that an open electrode design domain leads to thin shapes without convergence. When the design domain of the electrode was restricted, we attained solid shapes with convergence.

Although we used constraints on the design domain of the electrode to obtain the converged shapes, we could consider another method using a constraint on the boundary measure. However, this is left for future work.

A Formula of shape derivative

In Section 6, the following formula is used ([2] p. 96 Proposition 4.4).

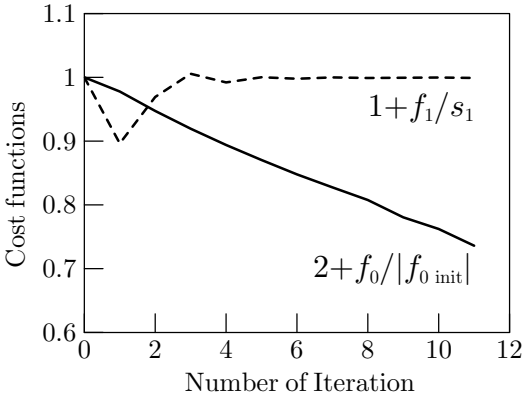

Fig. 13 Example 2a: Iteration history of cost functions

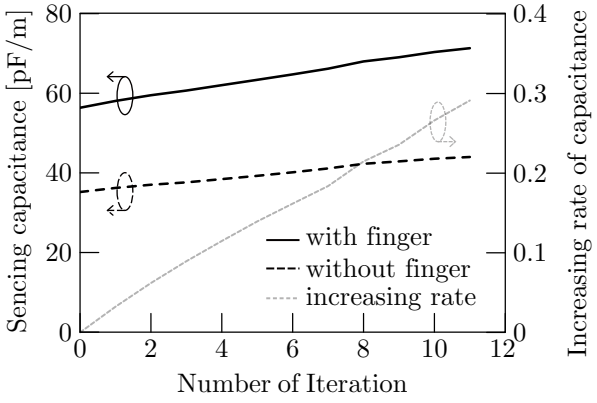

Fig. 14 Example 2a: Iteration history of sensing capacitance and rate of capacitance difference against initial shape

Proposition 1 (Shape derivative of domain integral)
Let $\boldsymbol{\phi} \in \mathcal{D}$, $u \in \mathcal{U} = C^1\left(\mathcal{D}; H^1\left(\mathbb{R}^d; \mathbb{R}\right)\right)$, $\boldsymbol{\nabla} u \in \mathcal{V} = C^1\left(\mathcal{D}; L^2\left(\mathbb{R}^d; \mathbb{R}^d\right)\right)$, and $h\left(u, \boldsymbol{\nabla} u\right) \in C^1\left(\mathcal{U} \times \mathcal{V}; L^2\left(\mathbb{R}^d; \mathbb{R}\right)\right)$. Writing $\boldsymbol{z} = \boldsymbol{x} + \boldsymbol{\varphi}\left(\boldsymbol{x}\right)$, let

$$
\begin{aligned}
&f\left(\boldsymbol{\phi} + \boldsymbol{\varphi}, u\left(\boldsymbol{\phi} + \boldsymbol{\varphi}\right), \boldsymbol{\nabla}_z u\left(\boldsymbol{\phi} + \boldsymbol{\varphi}\right)\right) \\
&= \int_{\Omega(\boldsymbol{\phi}+\boldsymbol{\varphi})} h\left(u\left(\boldsymbol{\phi} + \boldsymbol{\varphi}\right), \boldsymbol{\nabla}_z u\left(\boldsymbol{\phi} + \boldsymbol{\varphi}\right)\right) \mathrm{d}z
\end{aligned}
$$

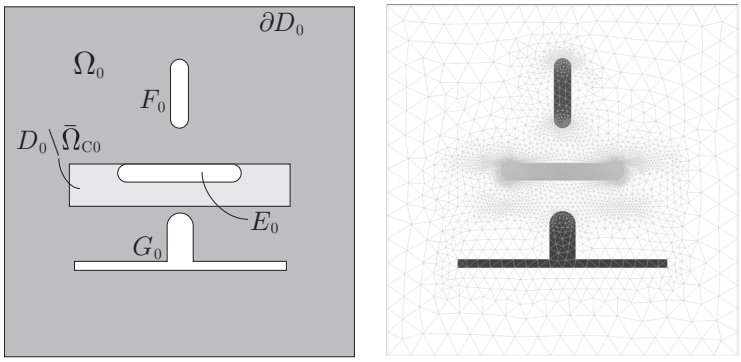

(a) Problem setting (b) Finite-element model

Fig. 15 Example 2b: Two-dimensional electrostatic field with protruding earth electrode

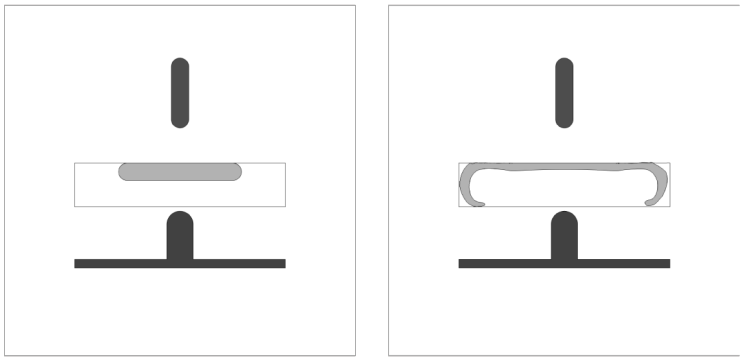

(a) Initial (b) Optimized (convergence)

Fig. 16 Example 2b: Shapes before and after domain variation

for an arbitrary $\boldsymbol{\varphi} \in \mathcal{D}$. Then, the shape derivative (Fréchet derivative with respect to domain variation) of f is given by

$$\begin{aligned} & f'\left(\boldsymbol{\phi}, u\left(\boldsymbol{\phi}\right), \boldsymbol{\nabla} u\left(\boldsymbol{\phi}\right)\right)[\boldsymbol{\varphi}] \\ & = \int_{\Omega(\boldsymbol{\phi})} \left\{ h_u\left(u\left(\boldsymbol{\phi}\right), \boldsymbol{\nabla} u\left(\boldsymbol{\phi}\right)\right)\left[u'\left(\boldsymbol{\phi}\right)[\boldsymbol{\varphi}]\right] \right. \\ & \quad + h_{\boldsymbol{\nabla} u}\left(u\left(\boldsymbol{\phi}\right), \boldsymbol{\nabla} u\left(\boldsymbol{\phi}\right)\right)\left[\boldsymbol{\nabla} u'\left(\boldsymbol{\phi}\right)[\boldsymbol{\varphi}] - \boldsymbol{\nabla}\boldsymbol{\varphi}^{\mathrm{T}} \boldsymbol{\nabla} u\left(\boldsymbol{\phi}\right)\right] \\ & \quad \left. + h\left(u\left(\boldsymbol{\phi}\right), \boldsymbol{\nabla} u\left(\boldsymbol{\phi}\right)\right) \boldsymbol{\nabla} \cdot \boldsymbol{\varphi} \right\} \mathrm{d}x, \end{aligned} \tag{A.1}$$

where $u'\left(\boldsymbol{\phi}\right)[\boldsymbol{\varphi}]$ is the shape derivative of $u\left(\boldsymbol{\phi}\right)$ with respect to $\boldsymbol{\varphi} \in \mathcal{D}$.

References

1. Azegami, H.: A solution to domain optimization problems. Trans. of Jpn. Soc. of Mech. Engs., Ser. A **60**, 1479–1486 (1994). (in Japanese)

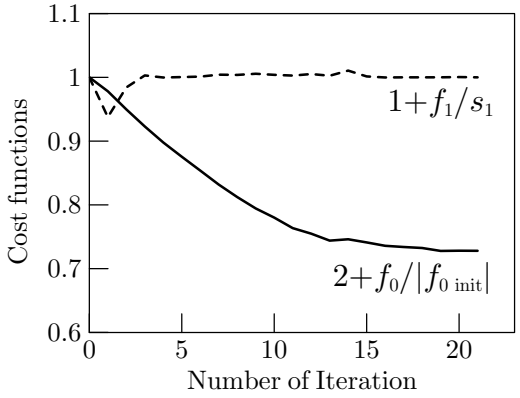

Fig. 17 Example 2b: Iteration history of cost functions

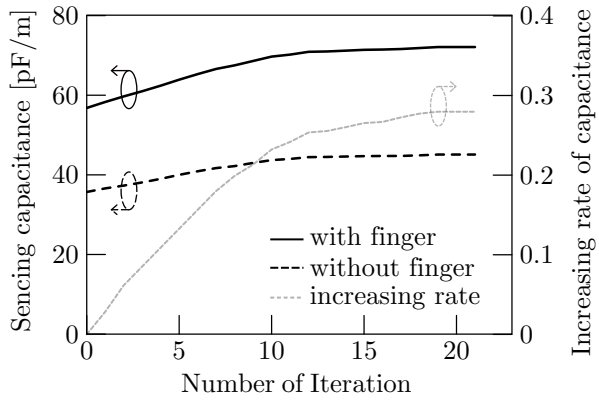

Fig. 18 Example 2b: Iteration history of sensing capacitance and rate of capacitance difference against initial shape

2. Azegami, H.: Regularized solution to shape optimization problem (in Japanese). Trans. JSIAM **24**(2), 83–138 (2014)
3. Azegami, H., Fukumoto, S., Aoyama, T.: Shape optimization of continua using nurbs as basis functions. Structural and Multidisciplinary Optimization **47**(2), 247–258 (2013)
4. Azegami, H., Kaizu, S., Takeuchi, K.: Regular solution to topology optimization problems of continua. JSIAM Letters **3**, 1–4 (2011)
5. Azegami, H., Ohtsuka, K., Kimura, M.: Shape derivative of cost function for singular point: Evaluation by the generalized j integral. JSIAM Letters **6**, 29–32 (2014). DOI 10.14495/jsiaml.6.29
6. Azegami, H., Takeuchi, K.: A smoothing method for shape optimization: traction method using the Robin condition. International Journal of Computational Methods **3**(1), 21–33 (2006)
7. Azegami, H., Zhou, L., Umemura, K., Kondo, N.: Shape optimization for a link mechanism. Structural and Multidisciplinary Optimization (2013). DOI 10.1007/s00158-013-0886-9
8. Crescini, D., Ferrari, V., Marioli, D., Taroni, A.: A thick-film capacitive pressure sensor with improved linearity due to electrode-shaping and frequency conversion. Mea-

surement Science and Technology **8**(1), 71 (1997). URL http://stacks.iop.org/0957-0233/8/i=1/a=010
9. Davison, B.: Techniques for robust touch sensing design. Application Note 1334, Microchip Technology Inc. (2010). URL http://ww1.microchip.com/downloads/en/AppNotes/00001334B.pdf
10. Du, L., Kwon, G., Arai, F., Fukuda, T., Itoigawa, K., Tukahara, Y.: Structure design of micro touch sensor array. Sensors and Actuators A: Physical **107**(1), 7 – 13 (2003). DOI http://dx.doi.org/10.1016/S0924-4247(03)00105-5. URL http://www.sciencedirect.com/science/article/pii/S0924424703001055
11. Kim, Y.S., Byun, J.K., Park, I.H.: A level set method for shape optimization of electromagnetic systems. Magnetics, IEEE Transactions on **45**(3), 1466–1469 (2009). DOI 10.1109/TMAG.2009.2012681
12. Kimura, M.: Shape derivative of minimum potential energy: abstract theory and applications. Jindřich Nečas Center for Mathematical Modeling Lecture notes Volume IV, Topics in Mathematical Modeling pp. 1–38 (2008)
13. Voorthuyzen, J.A., Sprenkels, A.J., van der Donk, A.G.H., Scheeper, P.R., Bergveld, P.: Optimization of capactive microphone and pressure sensor performance by capacitor-electrode shaping. Sensors and Actuafors A **25–27**, 331–336 (1991)